IEEE Access
Multidisciplinary | Rapid Review | Open Access Journal

Received April 25, 2019, accepted May 17, 2019, date of publication May 27, 2019, date of current version June 13, 2019.

Digital Object Identifier 10.1109/ACCESS.2019.2919265

Improving Wide-Angle Scanning Performance of Phased Array Antenna by Dielectric Sheet

GUANGWEI YANG, (Student Member, IEEE), QINGQING CHEN, JIANYING LI, (Member, IEEE), SHIGANG ZHOU, (Member, IEEE), AND ZIJIAN XING, (Member, IEEE)

School of Electrical and Information, Northwestern Polytechnical University, Xi'an 710129, China

Corresponding author: Jianying Li (jianyingli@nwpu.edu.cn)

This work was supported by the National Natural Science Foundation of China under 61871324.

ABSTRACT The method to improve the wide-angle scanning performance of the phased array antenna is studied and presented. The proposed method is realized by the dielectric sheet to reduce the size of the wide beam antenna and mutual coupling between the elements in the array antenna. The size of the antenna element is reduced by the dielectric sheet which is arranged on the top of the feed slot. The mutual coupling of the array antenna is improved by the dielectric sheet. And, the wide-angle impedance matching performance is improved by the above method. The operating frequency band of the E- and H-plane-phased array antennas is from 3.2 to 3.8 GHz. The main beams of the E-plane scanning array antenna can scan from $-90°$ to $+90°$ with the gain variation less than 3 dB. The main beams of the H-plane scanning array antenna can scan from $-70°$ to $+70°$ with the gain variation of less than 3 dB. The E- and H-plane scanning linear array antennas with nine elements are fabricated and tested. The measured results have a good agreement with the simulated results.

INDEX TERMS Phased array antenna, microstrip antenna, scanning antennas, wide beam antenna.

I. INTRODUCTION

With the rapid development of electronic technology, phased array antenna has been widely applied in satellite communication system, radar, astronomical meteorology, air traffic, earth exploration, space exploration, remote sensing mapping, 5G communication system, and so on in recent years because of the remarkable characteristics of the phased array are agile and flexible beam scan capacity, high tracking accuracy, and adapting to the high-speed maneuver capacity of the carrier. However, phased array antenna has a serious drawback which is the limited beam scanning range of the antenna with high gain [1]. For traditional phased array antennas, the main beams can scan from $-45°$ to $+45°$ with a gain fluctuation of 4-5 dB [2], because the beam-widths of the elements are limited, and mutual coupling between elements is strong when the beam is scanned at low elevation (near end-fire) angles. Actually, it cannot satisfy the demand above most application. In order to further extend the beam scanning coverage, many related efforts have been carried out to break the bottlenecks of limited scanning angles [3]–[26]. Firstly, the wide beam-width antenna element is applied in the phased array antenna to improve the wide-angle scanning performance [3]–[10]. A dual-band wide beam microstrip antenna element is presented in [3]. The half-power beam-width of the antenna in the low and high frequency band is $104°$ and $94°$ in the E-plane and $105°$ and $110°$ in the H-plane, respectively. A 9×9 planar phased array is designed with the proposed antenna elements and achieves the scanning range from $-60°$ to $+60°$ and $-50°$ to $+50°$ in the low and high frequency bands, respectively. A microstrip magnetic dipole antenna is applied to improve the wide-angle scanning performance of the array antenna in [4]. The 1×9 linear phased array is fabricated with the proposed antenna element and achieves the scanning range from $-76°$ to $+76°$ and $-64°$ to $+64°$ in the E-plane and H-plane linear array, respectively. Besides, some other wide beam antenna elements such as wide beam tapered slot antenna [5], quasi-hemispherical-pattern antenna [7], wide-beam substrate integrated waveguide (SIW)-slot antenna [9], resonant microstrip meander line antenna element [10] and a simple wide beam antenna elements [11], [12] are applied to improve the wide-angle scanning characteristic of the phased array antenna. Secondly, some technologies used to decrease or compensate the mutual coupling among the elements of the array antenna achieve wide-angle scanning phased array antenna [13]–[26]. A classic method is proposed in [13] and

The associate editor coordinating the review of this manuscript and approving it for publication was Guan-Long Huang.

2169-3536 © 2019 IEEE. Translations and content mining are permitted for academic research only.
Personal use is also permitted, but republication/redistribution requires IEEE permission.
See http://www.ieee.org/publications_standards/publications/rights/index.html for more information.

introduces a thin, high-permittivity dielectric sheet located at some distance above the array to achieve wide-angle impedance matching (WAIM). In recent years, some lecturers present some other methods [14]–[20] which are similar to the one in [13]. They utilize a sheet of split-ring resonators (SRRs) [14], a multilayer WAIM structure [15]–[17], a two-layer WAIM structure [18], a metamaterial slab [19], and a frequency select surface [20] to replace the dielectric sheet in [13] for realizing the wide-angle scanning capability of the array antenna. Besides, the defected ground structure (DGS) [21], [22], electromagnetic band gap (EBG) structure [23], high impedance surfaces (HIS) [24], [25], and substrate-integrated cavity-backed (SICB) structure [26] are applied to eliminate surface waves and improve WAIM. In addition, there are also some other technologies to improve wide-angle scanning performance of the phased array antenna such as pattern reconfigurable technology [27], multi-plane array technology [28], the varactor diode loading technology [29] and so on.

Combined with the wide beam method and WAIM technology, a simple and more effective solution is applied in this paper to achieve the wide-angle scanning phased array antenna. Firstly, to solve the high fluctuation gain of a phased array at large scanning angle, a wide beam antenna element is designed by a wide beam method [30]. The 3-dB beam-width of the wide beam antenna is 240° in the E-plane and 154° in the H-plane at 3.5 GHz. Secondly, the wide-angle scanning performance is affected by the input impedance matching of the antenna element. The wide-angle impedance matching is improved by the dielectric sheet arranged on the top of the feed slot which is very simple and different with the references [13]–[20]. Hence, a simple and effective method is proposed in this paper and applied to realize two wide-angle scanning array antennas. In the E-plane linear phased array antenna, the main beam of the antenna can scan from $-90°$ to $+90°$ with a gain fluctuation less than 3dB. And in the H-plane linear phased array antenna, the main beam of the antenna can scan from $-70°$ to $+70°$ with the gain variation less than 3dB.

The organization of the paper is as follows. In the second section, the antenna element is proposed and the miniaturized performance of the antenna element is realized by the dielectric sheet. In the third section, the wide-angle impedance matching is met by the dielectric sheet. The wide-angle scanning performance of the array antennas are analyzed, which demonstrates that the proposed method is beneficial to the wide-angle scanning performance of the phased array. The measured results and discussion are presented in the fourth section. Finally, a summary together with concluding remarks is presented.

II. THE OPTIMIZED DESIGN AND PERFORMANCE ANALYSIS OF THE PROPOSED ANTENNA ELEMENT

The exploded view of the proposed antenna element is shown in Fig. 1. The antenna element consists of the electric walls,

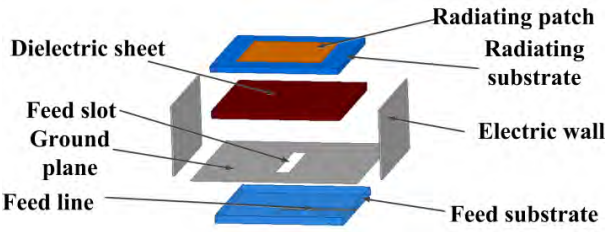

FIGURE 1. The exploded view of the proposed antenna element.

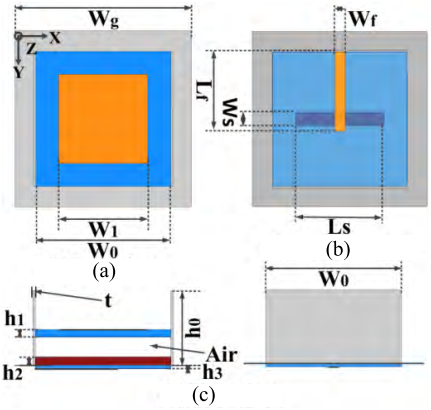

FIGURE 2. The diagram and parameters of the proposed antenna structure. (a) Top view. (b) Bottom view. (c) Side view.

the dielectric sheet, the microstrip radiation part and the slot coupling excitation part. The geometry of the antenna element is shown in the Fig. 2. The radiating patch and radiating substrate are in square shape, the side length of the patch is w_1 and the side length of the substrate is w_0, its thickness is h_1 and $\varepsilon_r = 2.2$. The feed substrate with a permittivity $\varepsilon_r = 2.2$ and a thickness h_3 is also a square with side length w_0. The feed slot is a rectangular structure with the length Ls and the width Ws. The length and width of the feed line is also a rectangular structure with the length L_f and the width W_f. The size of the electric walls is $h_0 \times W_0 \times t$. The size of the square dielectric sheet with a permittivity $\varepsilon_r = 3$ is the side length w_0, and the thickness h_2. The distance between the microstrip radiating part and the dielectric sheet is 5.0 mm.

The operating frequency band of the proposed antenna element is from 3.2 GHz to 3.9 GHz, as shown in Fig. 3. The electronic main beam steering is intended to cover a scan volume up to more than 60° in elevation plane for two scanning linear array antennas. In order to achieve an excellent wide-angle scanning performance of the array antenna, the element size needs to be reasonable small [31]. The minimum dimensions for the unit cell lattice are likewise determined by the achievable integration level. In the presented work, the dielectric sheet which is arranged on the top of the feed slot is used to reduce the element size. A more in-depth discussion about the detail function of the dielectric sheet will be presented in the next section. Comparing with the simulated reflection coefficients of the antenna element without

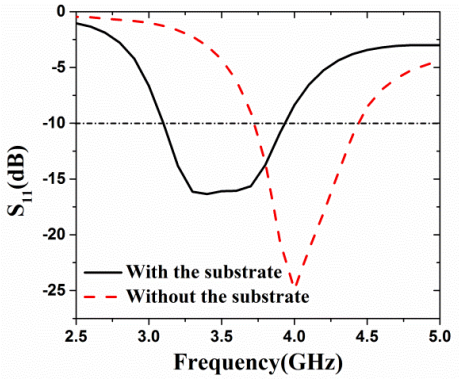

FIGURE 3. The simulated reflection coefficients of the antenna element with and without the dielectric sheet.

the dielectric sheet in the Fig. 3, the working frequency band is obviously reduced. On the other words, the size of the antenna element is reduced about 0.13 λ at the center frequency (3.5 GHz) by the dielectric sheet.

In addition, the wider beam-width of the antenna element is beneficial to the scanning phased array antenna [32]. The scanning coverage of the main beam of the array antenna expands using the wide beam-width array antenna element. In this paper, the electric walls which are arranged in the *xoz*-plane of the antenna are used to broaden the beam of the antenna element. Combined with the radiation theory of the microstrip antenna [30], the method to broaden the beam-width of the antenna element is as follows: the horizontal current is distributed in the radiating patch which producing the E-field. The vertical current is producing by the E-field and distributed in the electric walls. Through synthesizing the horizontal current and vertical current, the beam-width of the antenna element is broadened. The radiation patterns of the antenna element at 3.5 GHz are shown in Fig. 4. The half-power beam-widths of the antenna are 240° in the E-plane and 158° in the H-plane, respectively. The half-power beam-widths of the antenna are much wider than the aperture stacked patch antenna [33]. Since the half-power

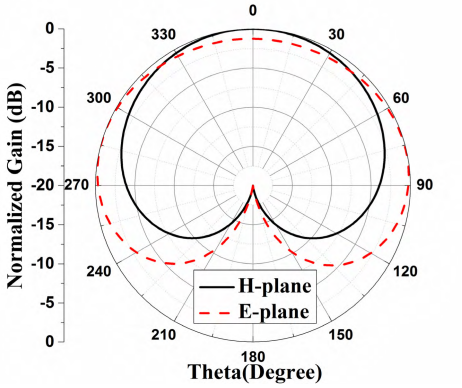

FIGURE 4. The simulated radiation patterns of the proposed antenna element.

beam-widths of the aperture stacked patch antenna are about 90° in the H-plane and 100° in the E-plane.

III. THE WIDE-ANGLE SCANNING PERFORMANCE OF THE ARRAY ANTENNAS

A. THE ARRAY ANTENNA GEOMETRY

As shown in Fig. 5 and Fig. 6, the E- and H-plane scanning array antennas are designed. Each of the array antennas composes of nine proposed wide beam elements. In contrast to the restructured antenna [34], it is simple to adequately perform the scanning beam range. The size of the ground plane is 350 mm × 40 mm. The height of the array antennas is 18 mm. The inter-element spacing is 36 mm, which is about 0.4 λ at 3.5 GHz.

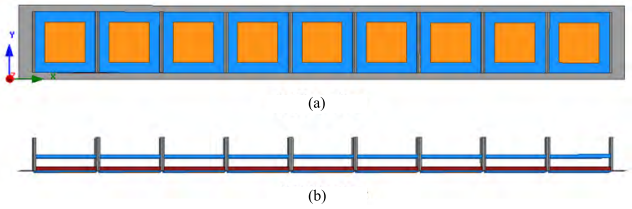

FIGURE 5. Geometry of the E-plane scanning phased array. (a) Top view. (b) Side view.

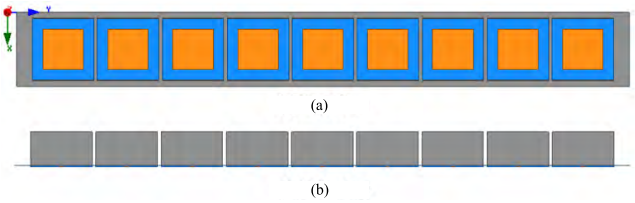

FIGURE 6. Geometry of the H-plane scanning phased array. (a) Top view. (b) Side view.

B. THE PERFORMANCE OF THE ARRAY ANTENNAS

The simulated and measured reflection coefficients of the E- and H-plane scanning array antennas are analyzed as shown in Fig. 7. The simulated and measured results are approximately in agreement. The impedance bandwidth is 3.18 – 3.95 GHz (21.6%) in the E-plane scanning array antenna and 3.18 – 3.90 GHz (20.3%) in the H-plane scanning array antenna.

To realize wide-angle scanning performance of the array antenna with the gain variation less than 3dB, the following conditions should be met. Firstly, the grating lobe of the array is disadvantageous to the main beam of the array antenna. So the grating lobe of the array must be suppressed. The condition for suppressing the grating lobe is

$$d < \frac{\lambda}{1 + |\sin\theta|}\left(1 - \frac{1}{2N}\right) \tag{1}$$

The inter-element spacing is d, and the scanning angle is θ. N is the number of the antenna elements. In this paper, the

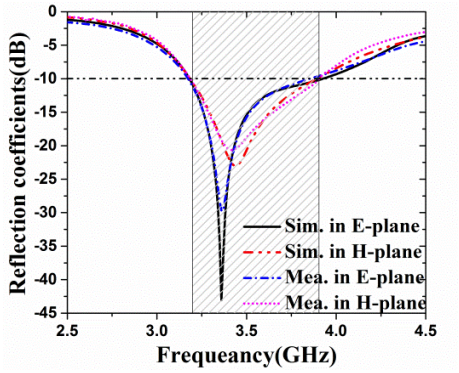

FIGURE 7. Measured and simulated reflection coefficients of the array antennas.

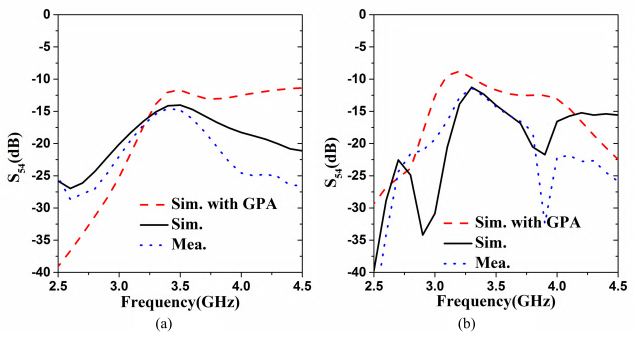

FIGURE 8. The reflection coefficients of the center element in the proposed array antennas and GPA at different scan angles. (a) E-plane. (b) H-plane.

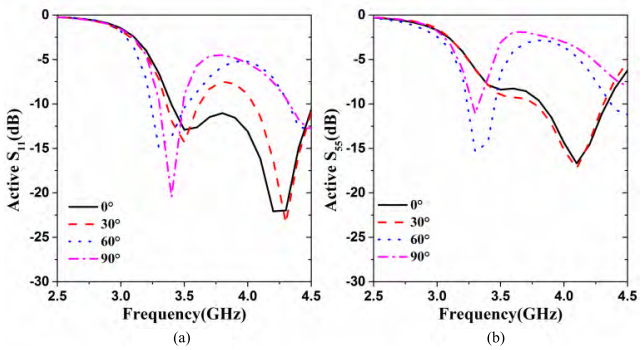

FIGURE 9. The active reflection coefficients of the elements in the E-plane GPA at different scan angles. (a) Element 1. (b) Element 5.

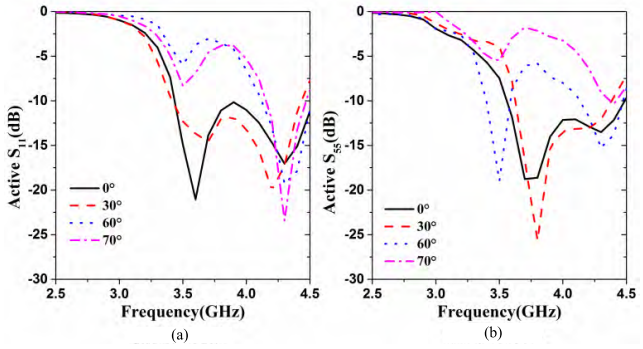

FIGURE 10. The active reflection coefficients of the elements in the H-plane GPA at different scan angles. (a) Element 1. (b) Element 5.

scanning angle is up to 90° and N is 9. Hence, the inter-element spacing is

$$d < \frac{\lambda}{1+|\sin\theta|}(1-\frac{1}{2N}) \approx 0.47\,\lambda \qquad (2)$$

In the above description of the paper, the antenna element size needs to be small as soon as possible. From Fig. 3, the size of the antenna element is shrunk by the dielectric sheet. The inter-element spacing is 36 mm, which is about 0.45 λ at 3.8 GHz. In the whole bandwidth, the inter-element spacing meets the Equation (2). Besides, the radiating patch of the element changes small, the mutual coupling of the antenna elements is reduced weakly when the inter-element spacing is constant. As shown in Fig. 8, the mutual coupling of the adjacent antenna elements is obviously improved by comparison with the general phased array antenna (GPA) without the dielectric sheet. In the E-plane array antenna, the coupling is reduced by at least 2.5 dB and reduced to −15dB in the operating frequency band. In the H-plane phased array, the coupling is reduced by at least 1.5 dB in the operating frequency band. Secondly, the antenna element should be a wide beam antenna. To guarantee that the array antenna scanning to wider coverage with the gain variation less than 3dB, the beam-width of the antenna element needs to be much wide. Hence, the beam of the wide beam antenna is broadened by the electric walls and used in the array antennas.

Thirdly, the wide-angle radiation performance needs to be enhanced. Generally, the wide-angle impedance matching performance is improved by the dielectric sheet which is arranged on the above antenna [13], [35]. In this paper, the dielectric sheet which is arranged on the ground plane is used to reduce the mutual coupling between the antenna elements in the array and improve the wide-angle impedance matching performance as shown in Fig. 1. To analyze the effect of the current method on wide-angle impedance matching of the antenna, the active reflection coefficients on the Element 1 and Element 5 in the array are given and compared with the elements in GPA. The active reflection coefficients of the elements at different scan angles in the E- and H- plane array antennas without the dielectric sheet is shown in Fig. 9 and Fig. 10. In the E-plane array antenna, the active reflection coefficients on the Element 1 and Element 5 are higher than −10 dB when the scan angle is up to 30 degrees in Fig. 9. In particular, the active reflection coefficients are higher than −5 dB when the scan angle is up to 60 degrees. The wide-angle impedance matching is not well when the scan angle is up to 30 degrees. In the H-plane array antenna, the active reflection coefficients on the Element 1 and Element 5 are higher than −10 dB when the scan angle is up to 60 degrees in Fig. 10. The wide-angle impedance matching is not well when the scan angle is up to 60 degrees. In the proposed array antennas, the wide-angle

impedance matching performance is obviously improved by the dielectric sheet as shown in Fig. 11 and Fig. 12. The active reflection coefficients on the Element 1 and Element 5 in the E-plane and H-plane array antennas are almost lower than −10 dB in the whole operating frequency band when the scan angle is up to 60 degrees. By comparing active reflection coefficients without and with the dielectric sheet, the wide-angle impedance matching performance is improved by the proposed method. Therefore, the dielectric sheet not only reduces the size of the antenna element, but also improves the wide-angle impedance matching performance.

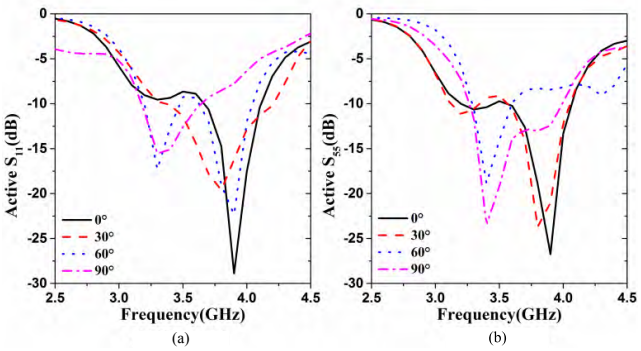

FIGURE 11. The active reflection coefficients of the elements in the proposed E-plane array at different scan angles. (a) Element 1. (b) Element 5.

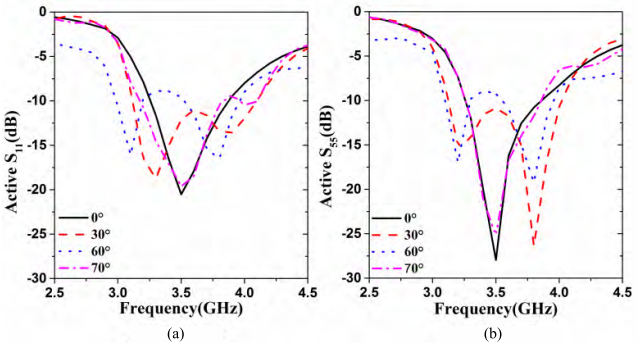

FIGURE 12. The active reflection coefficients of the elements in the proposed H-plane array at different scan angles. (a) Element 1. (b) Element 5.

C. THE SCANNING RADIATION PERFORMANCE OF THE E-PLANE ARRAY ANTENNA

The E-plane scanning array antenna is shown in Fig. 5. A parametric study and optimizing the scanning performance of the proposed array antenna have been carried out using Ansoft HFSS [36]. In the Fig. 13, the simulating radiation patterns of the above array antenna at three frequencies in the operating bandwidth are given. The beam of the antenna can realize to scan from −90° to +90° with the gain variation less than 3dB in the whole operating frequency band. The detailed scanning performance of the proposed antenna is given in Table 1. The gain of the proposed antenna gradually decreases with increasing the scanning angle of the beam. However, the scanning angle exceeds 60°, the gain of the antenna increases with variation of the scanning angle. In addition, the SLLs of the scanning beam are lower than 6.0 dB except the SLL of the scanning beam at 60°. The proposed method is applied to realize the wide-angle scanning capacity of the array antenna. The wide beam performance of the antenna element is realized by the electric wall. The wide-angle scanning impedance matching performance of the array antenna is improved by the dielectric sheet. In the whole work frequency band, the main beam of the proposed phased antenna can scan from broadside direction to endfire direction. Because the gain variation of the array antenna is less than 3 dB in the beam scanning coverage from −90° to +90°, the gain of the array antenna is not very high. When the scanning angles are ±60°, the gains of the array antenna are the least about 10.7 and 10.8 dBi at 3.2 GHz.

TABLE 1. The scanning radiation performance with different directions at different frequencies in the E-plane array.

Frequency (GHz)	3.2		3.5		3.8	
Steering Angle (deg)	Gain (dBi)	SLL (dB)	Gain (dBi)	SLL (dB)	Gain (dBi)	SLL (dB)
-90	12.8	-12.4	13.2	-12.2	12.8	-10.0
-60	10.7	-3.0	11.5	-5.0	12.5	-8.7
-30	12.2	-9.5	12.5	-8.1	13.1	-6.0
0	13.5	-13.4	14.1	-11.6	14.8	-11.2
30	12.2	-9.5	12.5	-8.2	13.0	-6.1
60	10.8	-3.0	11.6	-5.1	12.4	-8.8
90	12.7	-12.0	13.2	-13.1	12.8	-10.0

TABLE 2. The scanning radiation performance with different directions at different frequencies in the H-plane array.

Frequency (GHz)	3.2		3.5		3.8	
Steering Angle (deg)	Gain (dBi)	SLL (dB)	Gain (dBi)	SLL (dB)	Gain (dBi)	SLL (dB)
-70	9.8	-4.5	12.2	-7.4	13.8	-7.1
-60	12.0	-6.5	14.2	-8.5	15.6	-9.0
-30	11.5	-8.1	13.7	-10.6	15.2	-11.0
0	10.2	-6.8	12.8	-9.6	14.9	-10.7
30	11.4	-8.2	13.6	-10.5	15.1	-11.1
60	12.0	-6.6	14.2	-8.4	15.7	-9.2
70	10.0	-4.6	12.3	-7.5	14.2	-7.0

D. THE SCANNING RADIATION PERFORMANCE OF THE H-PLANE ARRAY ANTENNA

The H-plane scanning phased array is shown in Fig. 6. In the Fig. 14, the simulating radiation patterns of the above array antenna at three frequencies in the operating bandwidth are reported. The beam of the antenna can realize to scan from −70° to +70° with the gain variation less than 3dB in the whole operating frequency band. The detailed scanning performance of the proposed antenna is given in Table 2.

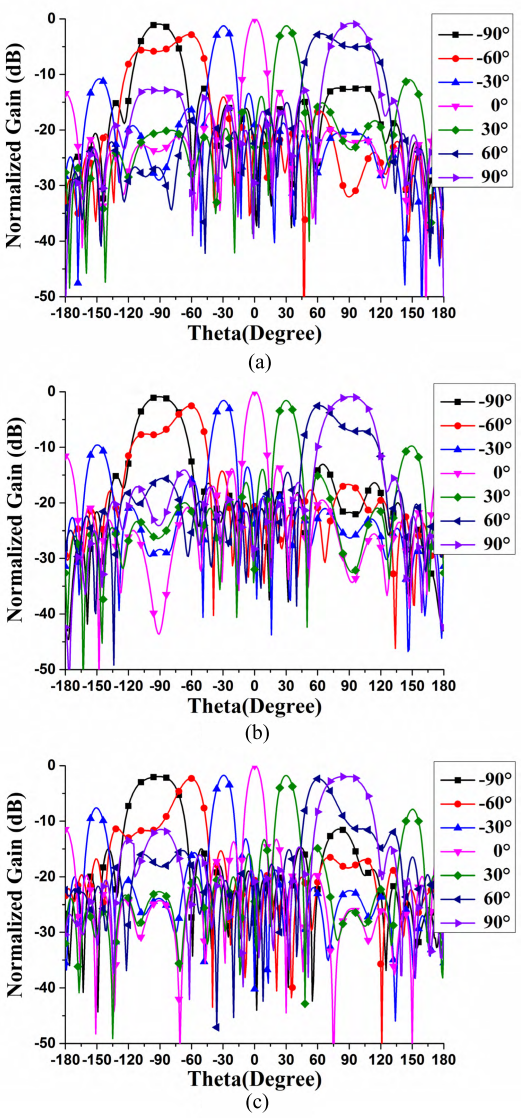

FIGURE 13. Scanning radiation performance of the E-plane scanning array antenna at different frequencies. (a) 3.2GHz. (b) 3.5GHz. (c) 3.8GHz.

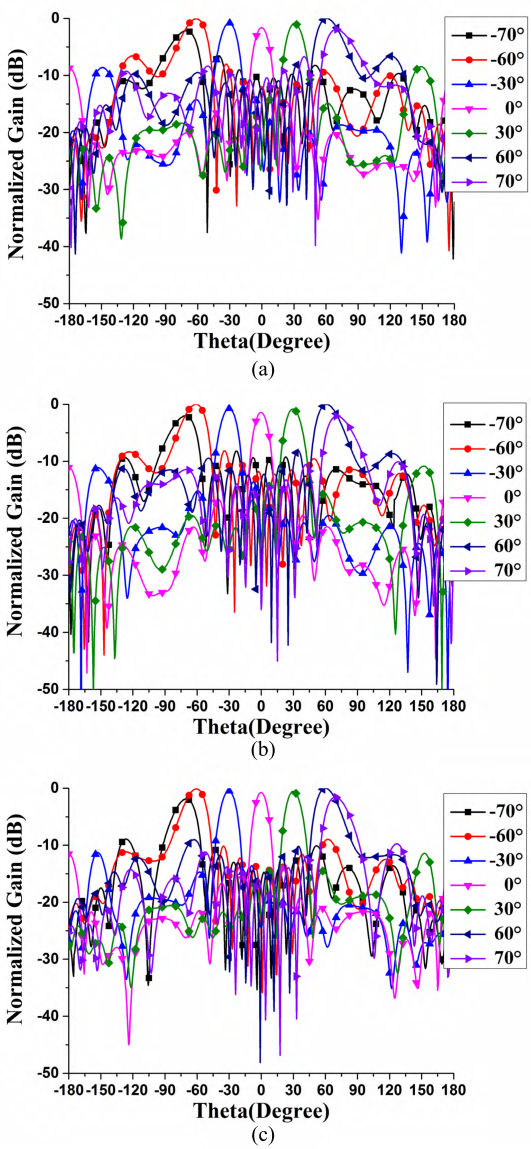

FIGURE 14. Scanning performance of the H-plane scanning array antenna at different frequencies. (a) 3.2GHz. (b) 3.5GHz. (c) 3.8GHz.

The gain of the proposed antenna gradually increases with increasing the scanning angle of the beam. However, the scanning angle exceeds 60°, the gain of the antenna decreases with variation of the scanning angle. In addition, the SLLs of the scanning beam are lower than 6.5dB except the SLL of the scanning beam at ±70° in the low frequency band. The proposed method is applied to realize the wide-angle scanning capacity of the array antenna. The wide beam performance of the antenna element is realized by the electric wall. The wide-angle scanning impedance matching performance of the array antenna is improved by the dielectric sheet. In the whole work frequency band, the beam of the proposed phased antenna can scan from −70° to +70° with the gain variation less than 3dB and lower SLLs. The side lobe levels of the H-plane scanning array in the operating bandwidth are better than the ones of the E-plane scanning array.

IV. MEASURED RESULTS

The E- and H-plane phased array antennas were fabricated for measurements as depicted in Fig. 15. In the figure, the E- and H-plane array prototypes are fabricated as the reference of the simulations using Ansoft HFSS. The size of the array prototype is consistent with the array antennas in Fig. 5 and 6. The antenna elements in the arrays are assembled and fixed by the nylon columns as shown in the Fig. 15. The scanning performance of the array antennas are verified and measured in the microwave anechoic chamber, shown in Fig. 16.

A. THE MEASURED SCANNING PERFORMANCE OF THE E-PLANE ARRAY ANTENNA

The measured radiation patterns at different frequencies in the E-plane array antenna are shown in Fig. 17. The measured radiation patterns of the E-plane array antenna are in

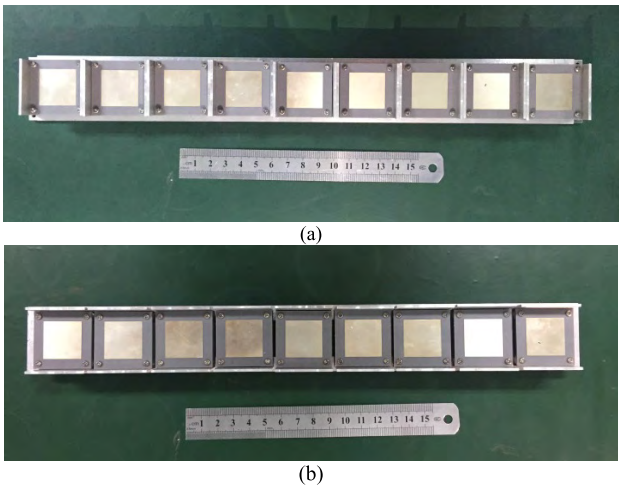

FIGURE 15. The array antenna prototype (a) The E-plane scanning array (b) The H-plane scanning array.

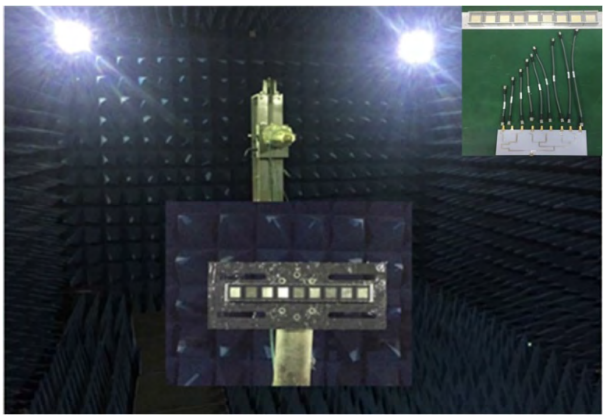

FIGURE 16. The testing picture in the microwave anechoic chamber.

good agreement with the simulated results in Fig. 13. The beam of the antenna can realize to scan from −90° to +90° with the gain variation less than 3dB in the whole operating frequency band. The detailed scanning performance of the proposed antenna is given in Table 3. The gain of the proposed antenna gradually decreases with increasing the scanning angle of the beam. However, the scanning angle exceeds 60°, the gain of the antenna increases with the variation of the scanning angle. In addition, the SLLs of the scanning beam are lower than 5.8dB except the SLL of the scanning beam at 60°. The simulated gains of the scanning beams are higher than the measured ones. And there are some slightly differences between the simulated SLLs and measured SLLs. It is mainly produced by the following factors. Firstly, there is some difference between the simulated and fabricated antenna. Secondly, it is most critical impact that the testing processing and environment is not ideal, as shown in Fig. 16. Thirdly, the ports of the elements in the array are affected by the feed network, which leads the measured SLLs to make weak. However, the outstanding wide-angle scanning phased array antenna is realized. And the method to realize the

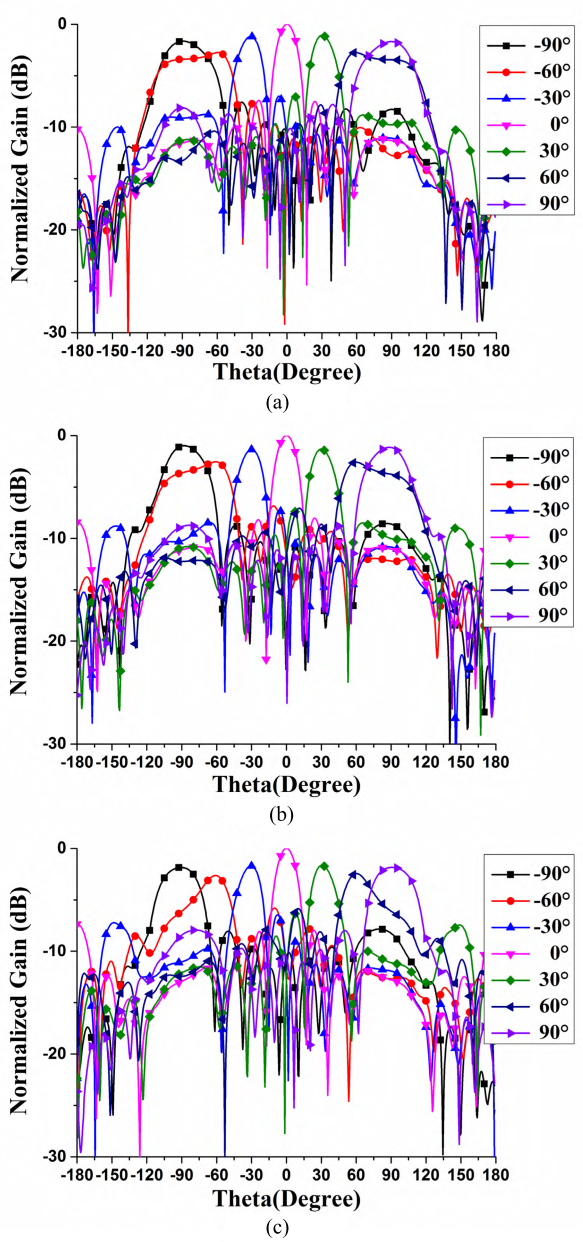

FIGURE 17. The measured radiation patterns of the E-plane scanning phased array at different frequencies. (a) 3.2GHz. (b) 3.5GHz. (c) 3.8GHz.

wide-angle scanning performance is verified by the proposed array antenna, which can scan its main beam over the range from −90° to +90° at 3.2, 3.5 and 3.8 GHz with high gain.

B. THE MEASURED SCANNING PERFORMANCE OF THE H-PLANE ARRAY ANTENNA

The measured radiation patterns in the H-plane array antenna at 3.2, 3.5 and 3.8 GHz are shown in Fig. 18. The measured radiation patterns of the H-plane array antenna are in good agreement with the simulated results in Fig. 14. The beam of the antenna can realize to scan from −70° to +70° with the gain variation less than 3dB in the whole operating frequency

TABLE 3. The scanning radiation performance with different directions at different frequencies in the E-plane array.

Angle(deg)			-90	-60	-30	0	30	60	90
3.2 (GHz)	Gain (dBi)	S	12.8	10.7	12.2	13.5	12.2	10.8	12.7
		M	11.2	10.1	11.6	12.8	11.7	10.0	11.1
	SLL (dB)	S	-12.4	-3.0	-9.5	-13.4	-9.5	-3.0	-12.0
		M	-5.4	-5.1	-5.8	-7.5	-5.8	-5.0	-5.0
3.5 (GHz)	Gain (dBi)	S	13.2	11.5	12.5	14.1	12.5	11.6	13.2
		M	12.3	10.7	11.9	13.3	12.0	10.7	12.2
	SLL (dB)	S	-12.2	-5.0	-8.1	-11.6	-8.2	-5.1	-13.1
		M	-7.8	-4.3	-5.9	-8.0	-6.0	-4.5	-7.7
3.8 (GHz)	Gain (dBi)	S	12.8	12.5	13.1	14.8	13.0	12.4	12.8
		M	12.1	11.3	12.3	14.0	12.3	11.5	12.1
	SLL (dB)	S	-10.0	-8.7	-6.0	-11.2	-6.1	-8.8	-10.0
		M	-6.2	-3.1	-5.5	-8.0	-6.0	-3.4	-6.3

TABLE 4. The scanning radiation performance with different directions at different frequencies in the H-plane array.

Angle(deg)			-70	- 60	- 30	0	30	60	70
3.2 (GHz)	Gain (dBi)	S	9.8	12.0	11.5	10.2	11.4	12.0	10.0
		M	8.5	9.9	10.1	9.5	10.0	9.9	8.6
	SLL (dB)	S	-4.5	-6.5	-8.1	-6.8	-8.2	-6.6	-4.6
		M	-3.3	-3.5	-6.0	-5.0	-6.0	-3.8	-3.5
3.5 (GHz)	Gain (dBi)	S	12.2	14.2	13.7	12.8	13.6	14.2	12.3
		M	11.0	12.6	12.8	12.0	12.7	12.5	10.9
	SLL (dB)	S	-7.4	-8.5	-10.6	-9.6	-10.5	-8.4	-7.5
		M	-4.0	-4.6	-6.5	-6.0	-6.6	-4.8	-4.2
3.8 (GHz)	Gain (dBi)	S	13.8	15.6	15.2	14.9	15.1	15.7	14.2
		M	13.0	14.6	14.7	14.2	14.6	14.5	13.2
	SLL (dB)	S	-7.1	-9.0	-11.0	-10.7	-11.1	-9.2	-7.0
		M	-4.1	-6.4	-6.2	-7.3	-6.1	-6.5	-4.2

band. The detailed scanning performance of the proposed antenna is given in Table 4. The gain of the proposed antenna gradually increases with increasing the scanning angle of the beam. However, the scanning angle exceeds 60°, the gain of the antenna decreases with variation of the scanning angle. The simulated gains of the scanning beams are higher than the measured ones. And there are some slightly differences between the simulated SLLs and measured SLLs. It is mainly produced by the following factors. Firstly, there is some difference between the simulated and fabricated antenna. Secondly, it is most critical impact that the testing processing and environment is not ideal, as shown in Fig. 16. Thirdly, the ports of the elements in the array are affected by the feed network, which leads the measured SLLs to make weak. However, the outstanding wide-angle scanning phased array antenna is realized. And the method to realize the wide-angle scanning performance is verified by the proposed array antenna, which can scan its main beam over the range from $-70°$ to $+70°$ at 3.2, 3.5 and 3.8 GHz with high gain and low SLL.

From the above analysis, it is obvious that the proposed method is applied to realize wide-angle scanning array antenna which make its main beam scans from the broadside

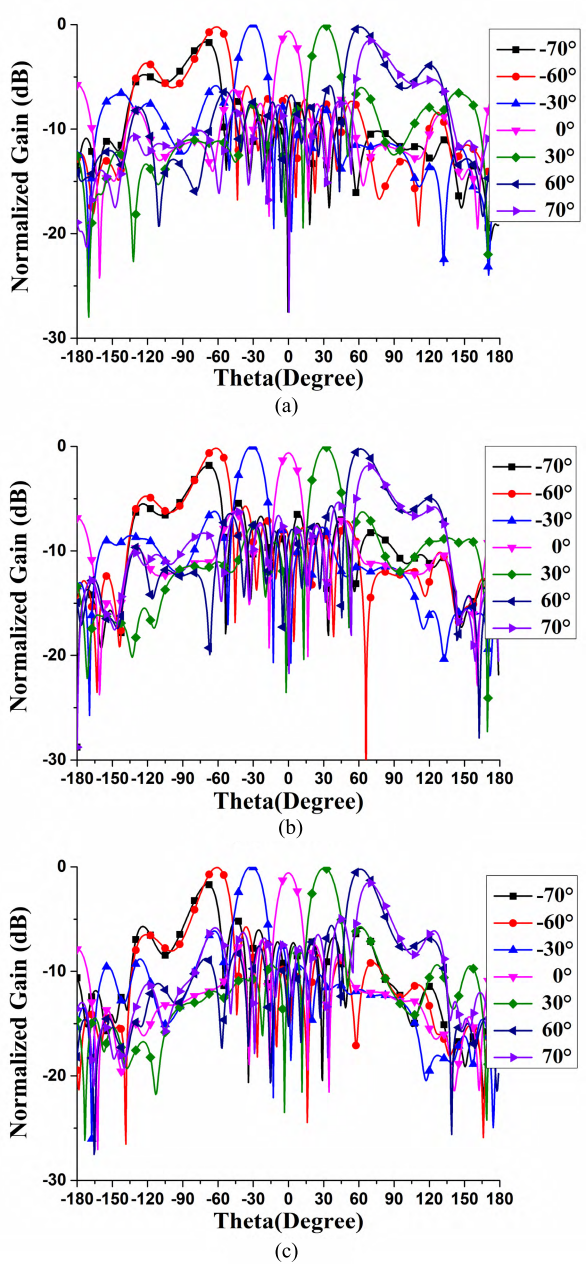

FIGURE 18. The measured radiation patterns of the H-plane scanning phased array at different frequencies. (a) 3.2GHz. (b) 3.5GHz. (c) 3.8GHz.

direction to the end-fire direction with the gain variation less than 3dB in the E-plane array antenna and from $-70°$ to $+70°$ with the gain variation less than 3dB in the H-plane array antenna in the bandwidth from 3.2 to 3.8 GHz, respectively. In addition, the dielectric sheet is beneficial to reducing the size of the elements and improving the wide-angle impedance matching performance of the phased array antenna.

V. CONCLUSION

In this paper, a miniaturization and wide beam aperture feed patch antenna is studied firstly. The antenna consists of the electric walls, the dielectric sheet, the feed part and the radiating part. The size of the antenna is reduced by the dielectric

sheet. The radiation beams can be improved in the E- and H- plane by the electric walls. The 3-dB beam-width is 240° in the E-plane and 154° in the H-plane at 3.5 GHz. Then, a simple method to realize the wide-angle scanning performance of the array antenna is proposed. The mutual coupling between the elements in the array antennas are improved in the E- and H- plane array antennas by comparison with the GPA. The wide-angle impedance matching performance is improved by the dielectric sheet. Hence, the main beam of the E- and H- plane scanning linear array antenna can scan from $-90°$ to $+90°$ and from $-70°$ to $+70°$ with the gain variation less than 3dB in the operating bandwidth from 3.2 to 3.8 GHz, respectively. The E- and H-plane scanning array antennas with nine elements are fabricated and tested. The measured results have a good agreement with the simulated results. In conclusion, an excellent wide-angle scanning performance from the broadside direction to the end-fire direction in the E-plane array antenna and from $-70°$ to $+70°$ in the H-plane scanning array antenna can be obtained by the proposed approach, which is can be applied to realize a planar wide-angle scanning phased array.

REFERENCES

[1] N. Amitay, V. Galindo, and C. P. Wu, *Theory and Analysis of Phased Array Antennas*. New York, NY, USA: Wiley, 1972.

[2] A. Neto, D. Cavallo, G. Gerini, and G. Toso, "Scanning performances of wideband connected arrays in the presence of a backing reflector," *IEEE Trans. Antennas Propag.*, vol. 57, no. 10, pp. 3092–3102, Sep. 2009.

[3] S. E. Valavan, D. Tran, A. G. Yarovoy, and A. G. Roederer, "Planar dual-band wide-scan phased array in X-band," *IEEE Trans. Antennas Propag.*, vol. 62, no. 10, pp. 5370–5375, Oct. 2014.

[4] C.-M. Liu, S.-Q. Xiao, H.-L. Tu, and Z. Ding, "Wide-angle scanning low profile phased array antenna based on a novel magnetic dipole," *IEEE Trans. Antennas Propag.*, vol. 65, no. 3, pp. 1151–1162, Mar. 2017.

[5] A. Kedar and K. S. Beenamole, "Wide beam tapered slot antenna for wide-angle scanning phased array antenna," *Prog. Electromagn. Res. B*, vol. 8, no. 1, pp. 235–251, 2011.

[6] S. E. Valavan, D. Tran, A. G. Yarovoy, and A. G. Roederer, "Dual-band wide-angle scanning planar phased array in X/Ku-bands," *IEEE Trans. Antennas Propag.*, vol. 62, no. 5, pp. 2514–2521, May 2014.

[7] R. Wang, B.-Z. Wang, C. Hu, and X. Ding, "Wide-angle scanning planar array with quasi-hemispherical-pattern elements," *Sci. Rep.*, vol. 7, no. 1, Jun. 2017, Art. no. 2729.

[8] H. Holter, T.-H. Chio, and D. H. Schaubert, "Experimental results of 144-element dual-polarized endfire tapered-slot phased arrays," *IEEE Trans. Antennas Propag.*, vol. 48, no. 11, pp. 1707–1718, Nov. 2000.

[9] Y.-Q. Wen, B.-Z. Wang, and X. Ding, "Wide-beam SIW-slot antenna for wide-angle scanning phased array," *IEEE Antennas Wireless Propag. Lett.*, vol. 15, pp. 1638–1641, 2016.

[10] K. S. Beenamole, P. N. S. Kutiyal, U. K. Revankar, and V. M. Pandharipande, "Resonant microstrip meander line antenna element for wide scan angle active phased array antennas," *Microw. Opt. Technol. Lett.*, vol. 50, no. 7, pp. 1737–1740, Jul. 2010.

[11] G. W. Yang, J. Y. Li, D. J. Wei, and R. Xu, "Study on wide-angle scanning linear phased array antenna," *IEEE Trans. Antennas Propag.*, vol. 66, no. 1, pp. 450–455, Jan. 2018.

[12] G. Yang, J. Li, S.-G. Zhou, and Y. Qi, "A wide-angle E-plane scanning linear array antenna with wide beam elements," *IEEE Antennas Wireless Propag. Lett.*, vol. 16, pp. 2923–2926, Oct. 2017.

[13] E. Magill and H. A. Wheeler, "Wide-angle impedance matching of a planar array antenna by a dielectric sheet," *IEEE Trans. Antennas Propag.*, vol. AP-14, no. 1, pp. 49–53, Jan. 1966.

[14] T. R. Cameron and G. V. Eleftheriades, "Analysis and characterization of a wide-angle impedance matching metasurface for dipole phased arrays," *IEEE Trans. Antennas Propag.*, vol. 63, no. 9, pp. 3928–3938, Sep. 2015.

[15] R. E. Collin, *Foundations for Microwave Engineering*, 2nd ed. New York, NY, USA: McGraw-Hill, 1992.

[16] E. Martini, G. M. Sardi, P. Rocca, G. Oliveri, A. Massa, and S. Macii, "Optimization of metamaterial WAIM for planar arrays," in *Proc. USNC-URSI Radio Sci. Meeting (Joint with AP-S Symp.)*, Lake Buena Vista, FL, USA, Jul. 2013, p. 86.

[17] L. Manica, M. Carlin, I. Malcic, G. Oliveri, and A. Massa, "Wideband multilayer WAIM design and optimization," in *Proc. 8th Eur. Conf. Antennas Propag. (EuCAP)*, The Hague, The Netherlands, Apr. 2014, pp. 2997–3000.

[18] B. Munk, R. Taylor, T. Durharn, W. Croswell, B. Pigon, R. Boozer, S. Brown, M. Jones, J. Pryor, S. Ortiz, J. Rawnick, K. Krebs, M. Vanstrum, G. Gothard, and D. Wiebelt, "A low-profile broadband phased array antenna," in *Proc. IEEE Antennas Propag. Soc. Int. Symp. (APS)*, Columbus, OH, USA, vol. 2, Jun. 2003, pp. 448–451.

[19] S. Sajuyigbe, M. Ross, P. Geren, S. A. Cummer, M. H. Tanielian, and D. R. Smith, "Wide angle impedance matching metamaterials for waveguide-fed phased-array antennas," *IET Microw. Antennas Propag.*, vol. 4, no. 8, pp. 1063–1072, Aug. 2010.

[20] E. Yetisir, N. Ghalichechian, and J. L. Volakis, "Ultrawideband array with 70ř scanning using FSS superstrate," *IEEE Trans. Antennas Propag.*, vol. 64, no. 10, pp. 4256–4265, Oct. 2016.

[21] D.-B. Hou, S. Q. Xiao, and B.-Z. Wang, L. Jiang, J. Wang, and W. Hong, "Elimination of scan blindness with compact defected ground structures in microstrip phased array," *IET Microw., Antennas Propag.*, vol. 3, no. 2, pp. 269–275, Mar. 2009.

[22] L. Gu, Y.-W. Zhao, Q.-M. Cai, Z.-P. Zhang, B.-H. Xu, and Z.-P. Nie, "Scanning enhanced low-profile broadband phased array with radiator-sharing approach and defected ground structures," *IEEE Trans. Antennas Propag.*, vol. 65, no. 11, pp. 5846–5854, Nov. 2017.

[23] F. Caminita, S. Costanzo, G. Di Massa, G. Guarnieri, S. Maci, G. Mauriello, and I. Venneri, "Reduction of patch antenna coupling by using a compact EBG formed by shorted strips with interlocked branch-stubs," *IEEE Antennas Wireless Propag. Lett.*, vol. 8, pp. 811–814, 2009.

[24] M. Li, S.-Q. Xiao, and B.-Z. Wang, "Investigation of using high impedance surfaces for wide-angle scanning arrays," *IEEE Trans. Antennas Propag.*, vol. 63, no. 7, pp. 2895–2901, Jul. 2015.

[25] G. Yang, J. Li, R. Xu. Y. Ma, and Y. Qi, "Improving the performance of wide-angle scanning array antenna with a high-impedance periodic structure," *IEEE Antennas Wireless Propag. Lett.*, vol. 15, pp. 1819–1822, 2016.

[26] M. H. Awida, A. H. Kamel, and A. E. Fathy, "Analysis and design of wide-scan angle wide-band phased arrays of substrate-integrated cavity-backed patches," *IEEE Trans. Antennas Propag.*, vol. 61, no. 6, pp. 3034–3041, Jun. 2013.

[27] X. Ding, B.-Z. Wang, and G.-Q. He, "Research on a millimeter-wave phased array with wide-angle scanning performance," *IEEE Trans. Antennas Propag.*, vol. 61, no. 10, pp. 5319–5324, Oct. 2013.

[28] N. H. Noordin, T. Arslan, B. Flynn, and A. T. Erdogan, "Low-cost antenna array with wide scan angle property," *IET Microw. Antennas Propag.*, vol. 6, no. 15, pp. 1717–1727, Dec. 2012.

[29] R. B. Waterhouse, "A novel technique for increasing the scanning range of infinite arrays of microstrip patches," *IEEE Microw. Guided Wave Lett.*, vol. 3, no. 12, pp. 450–452, Dec. 1993.

[30] G. Yang, J.-Y. Li, D. Wei, S. Zhou, and J. Yang, "Broadening the beam-width of microstrip antenna by the induced vertical currents," *IET Microw. Antennas Propag.*, vol. 12, no. 2, pp. 190–194, Feb. 2018.

[31] A. K. Bhattacharyya, *Phased Array Antennas: Floquet Analysis, Synthesis, BFNs and Active Array Systems* (Microwave and Optical Engineering). Hoboken, NJ, USA: Wiley, 2006.

[32] W. L. Stutzman and A. Gary Thiele, *Antenna Theory and Design*. Hoboken, NJ, USA: Wiley, 2012.

[33] K. Ghorbani and R. B. Waterhouse, "Dual polarized wide-band aperture stacked patch antennas," *IEEE Trans. Antennas Propag.*, vol. 52, no. 8, pp. 2171–2175, Aug. 2004.

[34] R. J. Mailloux, J. F. McIlvenna, and N. Kernweis, "Microstrip array technology," *IEEE Trans. Antennas Propag.*, vol. 29, no. 1, pp. 25–37, Jan. 1981.

[35] J. A. Kasemodel, C.-C. Chen, and J. L. Volakis, "Wideband planar array with integrated feed and matching network for wide-angle scanning," *IEEE Trans. Antennas Propag.*, vol. 61, no. 9, pp. 4528–4537, Sep. 2013.

[36] Ansys Corp. *HFSS: High Frequency Structure Simulator Based on the Finite Element Method*. [Online]. Available: http://www.ansys.com

GUANGWEI YANG (S'15) received the B.S. degree in electric information engineering and the M.S. degree in electromagnetic field and microwave technology from Northwestern Polytechnical University, Xi'an, China, in 2012 and 2015, respectively, where he is currently pursuing the Ph.D. degree in electronic science and technology. His recent research interests include microstrip antennas, wideband antennas, millimeter-wave array antennas, circularly-polarized antennas, base station antennas, phased array antennas, reconfigurable antennas, scanning antenna, and EM periodic structures. He also serves as a Reviewer for all the IEEE and IET journals related to antennas.

QINGQING CHEN received the B.Sc. degree in electronic science and technology from Northwestern Polytechnical University, Xi'an, China, in 2017, where she is currently pursuing the master's degree in electromagnetic field and microwave technology. Her recent research interests include microstrip antennas, reconfigurable antennas, circularly-polarized antennas, omnidirectional antennas, leaky wave antennas, and periodic structures.

JIANYING LI (M'15) received the B.Sc. degree in mathematics from Henan Normal University, Xinxiang, China, in 1986, and the M.Eng.Sc. and Ph.D. degrees in electromagnetic field and microwave technology from Xidian University, Xi'an, China, in 1992 and 1999, respectively.

From 1992 to 1996, he was with the Xi'an Electronic Engineering Research Institute, Xi'an, China, as a Research Engineer. From 1999 to 2004, he was with the Department of Electrical and Computer Engineering, National University of Singapore (NUS). He was a Postdoctoral Research Fellow and then a High Performance Computation for Engineered Systems (HPCES) Programmer with Singapore-MIT Alliance (SMA). From 2005 to 2010, he was with the Temasek Laboratories, National University of Singapore (NUS), where he was a Research Scientist. Since 2011, he has been with the School of Electronic and Information, Northwestern Polytechnical University. His current research interests include the fast algorithms and its applications to radar cross sections, the analysis and design of phased arrays, waveguide slot antennas, and microstrip antennas, and EM periodic structures.

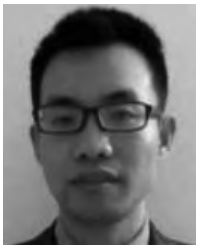

SHIGANG ZHOU received the B.Eng. and Ph.D. degrees in electronic engineering from Xidian University, Xi'an, China, in 2005 and 2010, respectively. From 2010 to 2013, he was with the Temasek Laboratories, National University of Singapore (TL@NUS), Singapore, as a Research Scientist. He is currently an Associate Professor with the School of Electronics and Information, Northwestern Polytechnical University (NWPU), Xi'an. His research interests include high-efficiency antenna arrays, wideband antenna arrays, multiband antenna arrays, phased arrays, broadband electrical small antennas, and numerical computation electromagnetics.

ZIJIAN XING was born in Gansu, China, in 1985. He received the B.Eng., M.Eng., and Ph.D. degrees from Northwestern Polytechnical University, China, in 2008, 2011, and 2014, respectively. In 2014, he was an Assistant Professor with Northwestern Polytechnical University, where he became an Associate Professor, in 2018. He has published over 10 SCI research papers. He was the Principal Investigator of three scientific research projects of antennas such as the National Natural Science Foundation of China. His research interests include circularly polarized antenna arrays, radio frequency identification circuits, and near-field antenna technology.